

# **Commissioning of the Mu2e Data AcQuisition system and the Vertical Slice Test of the straw tracker**

## **11. Mu2e ROC simulation**

version 1.0 October 23, 2023

### **Abstract**

This note presents the initial results of the tracker DAQ commissioning.

# Contents

<b>1</b>	<b>Notes for the authors</b>	<b>2</b>
1.1	Revision history . . . . .	2
<b>2</b>	<b>Introduction to the analysis</b>	<b>3</b>
<b>3</b>	<b>Monte Carlo simulation</b>	<b>3</b>
<b>4</b>	<b>Overflow mode: RUN281</b>	<b>4</b>
4.1	Time distribution . . . . .	4
4.2	nh vs ch . . . . .	4
4.3	nhits . . . . .	6
<b>5</b>	<b>buffer not full</b>	<b>7</b>
5.1	Time distribution . . . . .	7
5.2	nh vs ch . . . . .	7
5.3	nhits . . . . .	7
<b>6</b>	<b>rate</b>	<b>7</b>
<b>7</b>	<b>Summary</b>	<b>8</b>

# **1 Notes for the authors**

## **1.1 Revision history**

- v1.01: initial version

## 2 Introduction to the analysis

In this note, we present an analysis of the data derived from the readout teststands of the motherboard. This analysis was performed with the aim of characterizing the functionality of the Data Acquisition (DAQ) system. A signal generator was employed to send pulses and we tried to understand the output and non-output of the DTC. Our study centered on testing the performance of ROCs and DTCs, actually we were reading 1 ROC (96 channels), which is the equivalent of one panel or 2 ROCs. The analysis was executed employing a single DTC. During the analysis, we had the capability to change different generator's features. We varied the event window duration between successive pulses and modulated the generator's operating frequency. Specifically, we could operate with two distinct frequencies:  $31.29 \text{ MHz}/(2^7+1)$ , resulting in approximately 250 kHz, and  $31.29 \text{ MHz}/(2^9+1)$ , 60 kHz.

The selection of the event window duration and the frequency played an important role in determining the number of hits per event, considering that the ROC buffer possessed a storage capacity for up to 255 hits. The relationship between the generator and readout counts can be summarized as follows:

- $N_{gen} < 255$ :  $N_{readout} = N_{gen}$ ;
- $N_{gen} \geq 255$ :  $N_{readout} = 255$ .

## 3 Monte Carlo simulation

To ensure a comprehensive understanding of our system, we initiated a Monte Carlo Simulation of our Data Acquisition (DAQ) system. Given that the maximum allowable number of hits per event is 255, the simulation protocol adheres to the following sequential steps:

- Within a time interval ranging from  $0 \mu\text{s}$  to the reciprocal of the generator frequency, we generated the first event ( $t_0$ ) by following a uniform distribution;
- After verified that hits from the same channel, are separated by an interval equivalent to the reciprocal of the generator frequency, we proceeded to generate the second event ( $t_1$ ) by summing this specific time increment to  $t_0$ ;
- Subsequently, we verified whether the second pulse remained within the predefined time window. If it did, we included this hit in the ongoing event under construction;
- The process of event creation continued until the count of hits reached the maximum threshold of 255, at which point the event construction was terminated.

Furthermore, the simulation accounts for the channel to channel and FPGA to FPGA delays. This comprehensive approach ensures a faithful representation of the real-world operational aspects of the DAQ system.

## 4 Overflow mode: RUN281

### 4.1 Time distribution

The analysis started examining the data time distribution of each channel. After a preliminary observation of the distributions, we saw different patterns for channels in the first FPGA and in the second FPGA, as illustrated in Fig. 1: the initial though was the occurrence of a cessation in data acquisition for specific channels at a certain time.

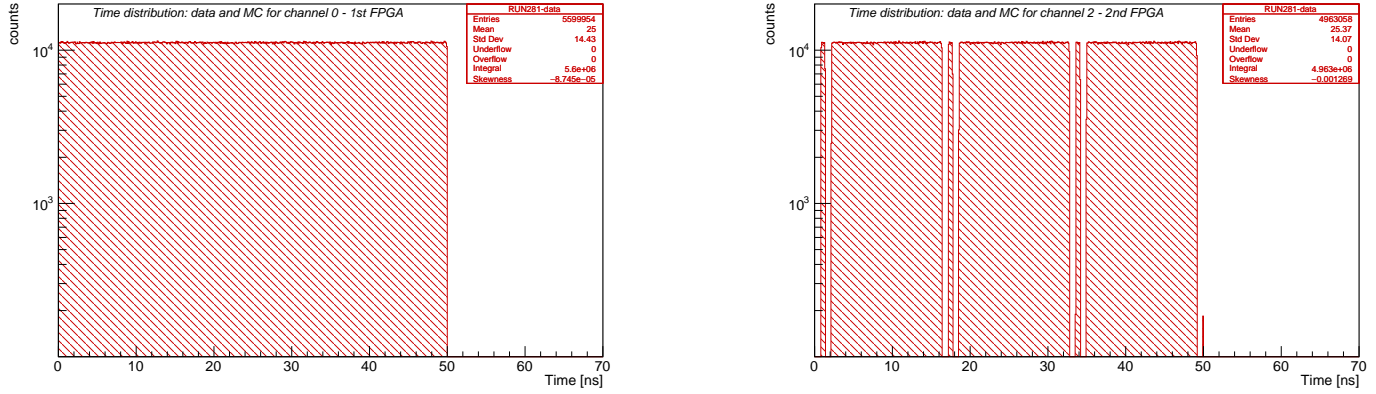


Figure 1: right: First FPGA's channel time distribution, left: Second FPGA's channel time distribution.

We thought it was necessary to characterize the apparatus with a Monte Carlo simulation for our Data Acquisition (DAQ) system, in order to understand the interruptions, so we redirect to section 3 for further information.

### 4.2 Occupancy: Number of hits versus channel

We conducted an analysis by plotting the number of hits in each channel as a function of the channel number, which revealed a non-uniform distribution. Specifically, channels were arranged in an ascending order, spanning from channel 0 to channel 95. As second step, we managed to generate a histogram with an alternative channel order, as we would expect the filling to occur. Our expectation was to observe a declining trend in the number of hits per channel, primarily due to the progressive filling of the buffer. However, contrary to our initial hypothesis, we encountered a distinctive pattern in which the number of hits exhibited a decrease until reaching zero hits at a specific channel, followed by a subsequent increase beyond the 72nd channel, which corresponds to channel 95.

Upon careful examination, we deduced that the initial channel ordering was incorrect. The first and the second lanes of the second FPGA were inverted and also some channels of the second FPGA. Consequently, we have identified a revised channel sequence, verified also by the Monte Carlo simulation, which is as follows:

**FIST FPGA:**

lane 1: 91,85,79,73,67,61,55,49,  
43,37,31,25,19,13,7,1,  
90,84,78,72,66,60,54,48,  
  
lane 2: 42,36,30,24,18,12,6,0,  
93,87,81,75,69,63,57,51,  
45,39,33,27,21,15,9,3,

**SECOND FPGA:**

lane 1: 38,44,5,11,17,23,29,35,  
41,92,2,8,14,20,26,32,  
86,80,74,68,62,56,50,47,  
  
lane 2: 95,89,83,22,16,28,34,40,  
46,53,59,65,71,77,10,4,  
94,88,82,76,70,64,58,52

At this point we have plotted the number of hits versus the channel number in the order that the filling occurred, as we can see in Fig. 2. We can see a perfect adherence between data and simulation. We

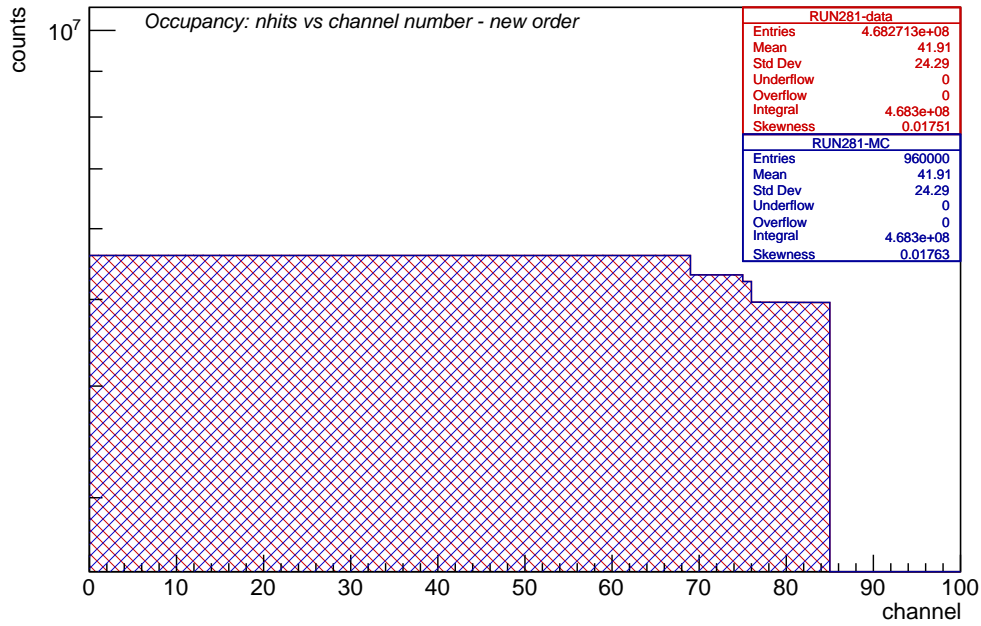


Figure 2: Occupancy: number of hits versus channel. The ordering of channels adheres to the sequence prescribed by the Monte Carlo simulation.

can interpret the histogram as it follows: the initial group of channels in the histogram, corresponds to the ones in which we accumulate 4 hits (associated with the first FPGA) and 3 hits (associated with the second FPGA). Subsequently, we observe a contrasting group of channels where the pattern reverses, 3 hits from the first FPGA followed by 4 hits from the second FPGA. We can observe a little jump in the middle and it is due to channel to channel time differences. Time differences between channels are three order of magnitude less than the FPGA ones, so these little jumps are very few, in our case only one appears. Lastly, the concluding cluster of channels is comprised of those collecting 3 hits from the first FPGA and 3 hits from the second FPGA.

### 4.3 Number of hits

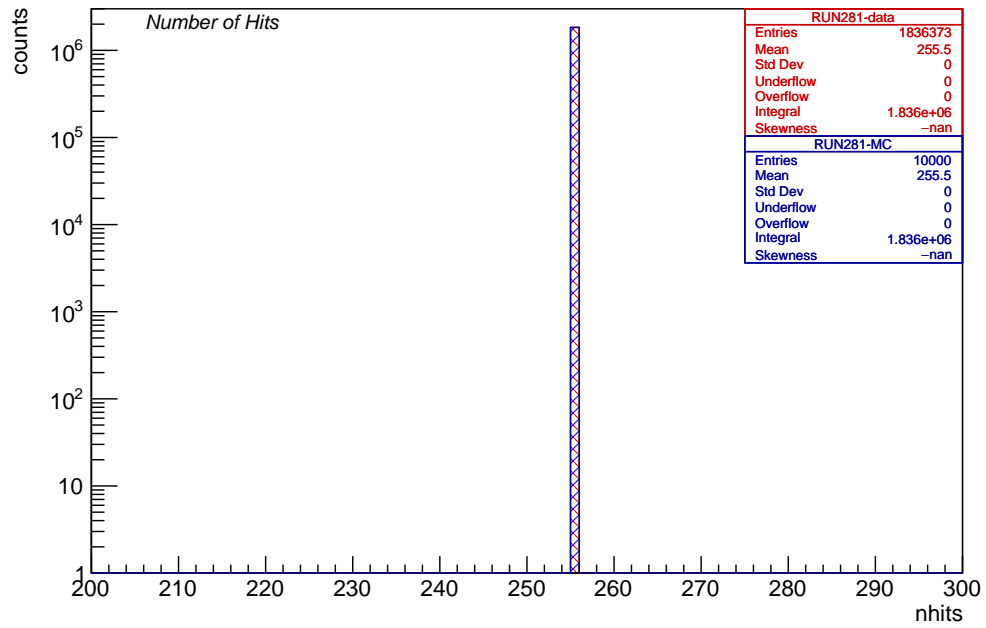


Figure 3: Number of hits distribution.

## **5 buffer not full**

### **5.1 Time distribution**

### **5.2 nh vs ch**

### **5.3 nhits**

## **6 rate**



## 7 Summary

Upper bounds on the direct beam-related backgrounds are as follows:

- background from beam electrons scattered in the stopping target  $< 1 \times 10^{-3}$
- background from muon decay in flights  $< 1 \times 10^{-3}$
- background from beam muons scattered in the stopping target  $< 1 \times 10^{-5}$